Design & Implementation Of Stand Alone High Gain Jammer system Against UAV Using Helical Antenna

Prof. Dr. Mamdouh Gouda
Misr University For Science and Technology
Head of Electronics and Communication Department
6 October, Giza
mamdouh.goda@must.edu.eg

Dr. Ashraf Mostafa Samy
Misr University For Science and Technology
6 October, Giza
ashraf.samy@must.edu.eg

Eng.M.A.Alim
Misr University For Science and Technology
6 October, Giza
moahmed.abdelaleem@must.edu.eg

Anas Mohamed
Misr University For Science and Technology
Department of electronics and communication engineering
6 October, Giza
80747@must.edu.eg

Adel Mahmoud Mohamed
Misr University For Science and Technology
Department of electronics and communication engineering
6 October, Giza
91620@must.edu.eg

Mahmoud Talaat Farag
Misr University For Science and Technology
Department of electronics and communication engineering
6 October, Giza
91621@must.edu.eg

Mohamed abdalrady Ebrahim
Misr University For Science and Technology
Department of electronics and communication engineering
6 October, Giza
91636@must.edu.eg

Passant Nagi Mourice
Misr University For Science and Technology
Department of electronics and communication engineering
6 October, Giza
91255@must.edu.eg

Rana Adel Mohamed
Misr University for Science and Technology
Department of electronics and communication engineering
6 October, Giza
91300@must.edu.eg

Merna Baher Badry
Misr University for Science and Technology
Department of electronics and communication engineering
6 October, Giza
91400@must.edu.eg

Rawan Mahmoud
Misr University for Science and Technology
Department of electronics and communication engineering
6 October, Giza
91630@must.edu.eg

Abstract— This researc **Abstract— This research presents a novel standalone high-gain jammer system designed to disrupt unmanned aerial vehicles (UAVs) operating on GNSS frequencies. The system utilizes four strategically placed helix antennas to achieve broad frequency coverage and employs a YOLO-based tracking system for accurate jamming. To ensure continuous operation, a solar-powered standby system provides reliable backup for the tracking unit. Experimental evaluations demonstrate the effectiveness of the system in disrupting UAVs, highlighting its potential to enhance security in sensitive areas and protect critical infrastructure. This research contributes to the field of UAV countermeasures by offering a practical and efficient solution for mitigating the growing threat posed by unauthorized drone activity**.

Keywords—GNSS, UAV, Jamming, AI, YOLO

I. INTRODUCTION

Diverse drone models are available in the consumer market, ranging from units designed for recreational sports and entertainment to sophisticated devices engineered for intricate operations. While drones can be utilized in conjunction with favorable legislation, even those with rudimentary capabilities may be exploited for nefarious purposes in contexts that society deems unacceptable or detrimental. For instance, basic drones might be employed by paparazzi to infringe upon the privacy of public figures or by malefactors and terrorists to jeopardize the safety of specified targets.

Consequently, alongside drone advancement, a variety of counter-drone mechanisms have also been established [1].

The foremost goal of this research is to conceptualize, construct, and appraise an independent jamming apparatus that can effectively neutralize Unmanned Aerial Vehicles (UAVs) operating within the Global Navigation Satellite System (GNSS) frequency spectrum using helical antennas. This study endeavors to furnish autonomous jamming solutions and contribute to the domain of drone security. Furthermore, it seeks to foster dialogue regarding the ethical deployment and governance of jamming systems operating within the GNSS frequency band, while examining the potential of helical antennas and their integration.

II. RELATED WORK SELECTING A TEMPLATE

J. has investigated the jamming efficacy of low-cost, commercially accessible jammers against UAVs. Farlik et al. (2016) where The GNSS signal can be jammed from a great enough distance, it is concluded. several hundred meters away from the UAV). However, the study discovers that using the proposed jammers to block the remote control signals is ineffective, even when the jammer is significantly closer to the UAV than the pilot

using the remote controller and We also have various modules with a wide bandwidth. For example, the AH-1117-13 is designed to deliver wideband directional transmission/reception of radio signals from 1100-1700 MHz bands, including GPS L1, GPS L2, L5, and Lo bands. It uses longer stubs to provide a better gain while keeping a larger beam-width.

Circular Polarization Antenna Technology, which provides improved penetration through obstruction and interference, is used in these low-profile antennas. There are helical antenna variants that are Right Hand Circular Polarized (RHCP) and Left Hand Circular Polarized (LHCP) [2]. Since there are various sorts of drones available in the consumer market, ranging from sports and entertainment to high-end machines capable of performing sophisticated tasks. Alongside the development of drones, different anti-drone devices have also been created.

The case where a radio-controlled drone enters an anti-drone system's active zone is examined in our study. Using their own unacquired photos, Sarah Kentsch et al. (2020) investigated and quantified difficulties pertaining to the usage of deep learning (DL) in forestry applications, including the impact of transfer learning (TL) and deep learning architecture. They focused on two distinct issue formalizations (Multi-Label)Patch or MLP classification and semantic segmentation), two in-house datasets (winter and coastal forest), and two distinct Deep Learning architectures (ResNet50 and UUNet).

The patch-based framework's compatibility with the ResNet50 architecture was demonstrated by the detection of the invasive broadleaf deciduous black locust (Robinia pseudo acacia) in an evergreen coniferous black pine (Pinus thunbergii) coastal forest typical of Japan. This was a more intricate and involved example. In this instance, we identified 75% of the photos as True Positives (TP) and 9% as False Positives (FP) containing the invasive species, whereas native tree recognition yielded 95% TP and 10% FP. [3] However, Min-Fan Ricky Lee et al. (2023) suggested a way to get over a number of problems, including uncertainty due to changes in occlusion, illumination, season, and views.

They applied various complex and uncertain environment scenarios are applied to evaluate the proposed system via the deep learning model's prediction metrics (accuracy, precision, recall, P-R curve, F1 score). The tracking rate based on the Siamese Region Proposal Network Algorithm is up to 180 FPS [4].

Tanvir Ahmad et al. (2020) Proposed a modified YOLOv1-based neural network is proposed for object detection. The following are some ways that the new neural network model has been enhanced. First, changes are made to the YOLOv1 network's loss function. The proportion style takes the place of the margin style in the updated model.

In terms of optimizing the network error, the new loss function is more reasonable and adaptable than the previous one. Thirdly, an inception model with a convolution kernel of 1 1 is introduced, hence reducing the number of weight parameters of the layers. Secondly, a spatial pyramid pooling layer is added. Extensive experiments using Pascal VOC datasets conducted between 2007 and 2012 showed that the recommended method enhanced performance [5].

Joseph Redmon, Santosh Divvala, Ross Girshick, and Ali Farhadi's book "You Only Look Once: Unified, Real-Time Object Detection". This paper introduces YOLO, a novel approach to object detection that frames it as a regression problem. With the base YOLO model processing images in real-time at 45 frames per second, the unified architecture operates at a very high speed. A smaller version, Fast YOLO, achieves an astounding 155 frames per second while maintaining double the mAP (mean average precision) of other real-time detectors.

[6] "A novel finetuned YOLOv6 transfer learning model for real-time object detection" proposes a pruning and fine-tuning algorithm along with transfer learning to enhance the efficiency of the YOLOv6 model in terms of detection accuracy and inference speed [7]. "Real-time object detection and segmentation technology: an analysis of the YOLO algorithm" explores the YOLO algorithm's development and its significance in real-time object detection and segmentation. [8]

III. MATERIALS AND METHODS

A. *Drone Model*

Insights into developing effective countermeasures against unauthorized drone activities while ensuring that legitimate GNSS services are maintained More than thirty percent of the receiver models utilized for drone applications currently have Galileo installed. There will be more drone users than any other GNSS user base in aviation due to the growing drone market, which will present new commercial prospects for application developers, based on a White Paper published by the European GNSS Agency on European Global Navigation Satellite Systems (EGNSS) for drone operations Drones now require GNSS; it's no longer an optional feature. Drone safety and dependability depend on global navigation satellite systems (GNSS), which are installed as standard equipment on nearly all new commercial drones. The most obvious option for navigation technology, though not the only one, is GNSS, perhaps with different augmentations, given the growing demand for beyond visual line of sight (BVLOS) operations. EGNSS for increased precision It should come as no surprise that Galileo is already found in more than 30% of drone receivers, as many of them also use EGNOS corrections to boost accuracy, given the extra accuracy that Galileo provides. An overview of the benefits of EGNOS and Galileo for both emergent and present operations, as well as for future U-Space

services, is given in the GSA White paper. [9]

B. Jammer Model System

Design of Helical Antenna and Specifications

The helix antenna functions similarly to an N-turn spring with a reflector. The circumference (C) of a turn is approximately one wavelength (λ), and the distance (d) between the turns is approx. 0.25C. The size of the reflector (R) is equal to C or λ and can be a circle or a square. Depending on how the helix is wound, the design produces circular polarization (CP), which can be either "right hand" or "left hand" (RHCP or LHCP, respectively). Unless a (passive) reflector is used in the radio route, both ends of the link must use the same polarization for optimal energy transfer.

The gain (G) of the antenna, relative to an isotope (dBi), can be estimated by:

(G) = (10.8+10 x log (number of turns x space between coils))

Diameter (D) = wavelength/3.143

Space between coils (S) = Space between coils x wavelengths

Length of wire (L) = Number of turns x √ (wavelength^2 + Space between coils^25

Half Power Beam Width of antenna = 52 / (√ (Number of turns x space between coils))

Beam Width First Nulls of antenna = 115 / (√ (Number of turns x Space between coils))

Aperture = (10(Antenna Gain / 10) x wavelength^2) / (4 * 3.14)

The Antennas Design & Calculations

1-For 1575.42 MHZ Helix

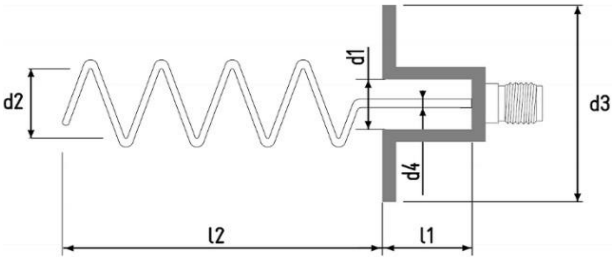

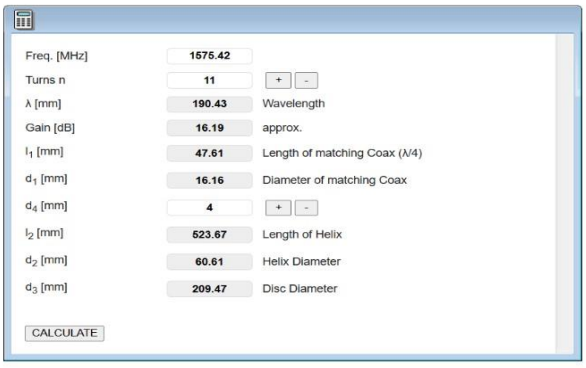

Fig1. the calculation of 1575.42 MHZ

Parameters of the matching transformer 140/50 Ω

- Triangle length L: 133 mm
- Triangle Height W: 40 mm

2-for 1195.192 MHz Helical Antenna

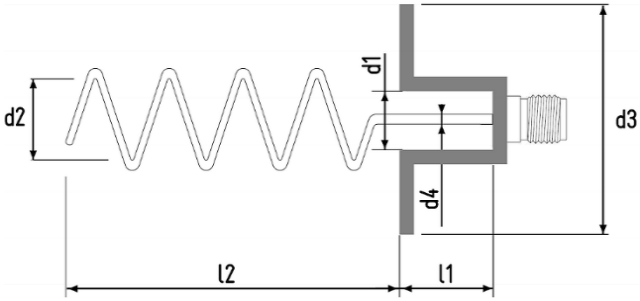

Fig2. the calculation of 1195.192 MHZ

Parameters of the matching transformer 140/50 Ω

- Triangle length L: 176 mm
- Triangle Height W: 52.7 mm

Note: And we make another 2 antennas by the same way.

1-The Results of the 1575.42 MHZ Helix

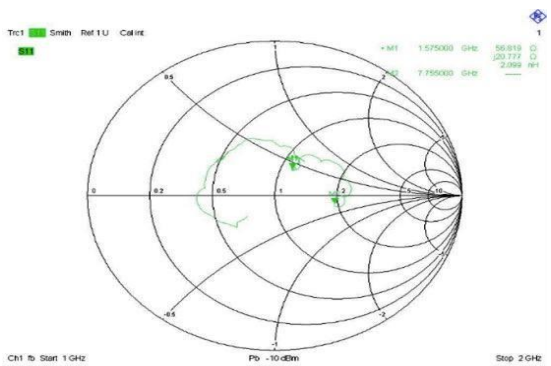

Fig3. smith chart of 1575.42 MHZ Antenna

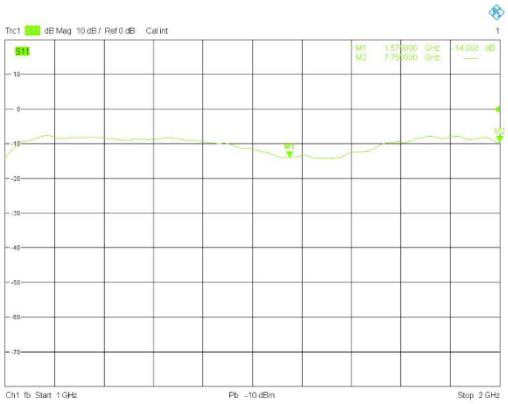

Fig4. return loss 1-2 GHZ

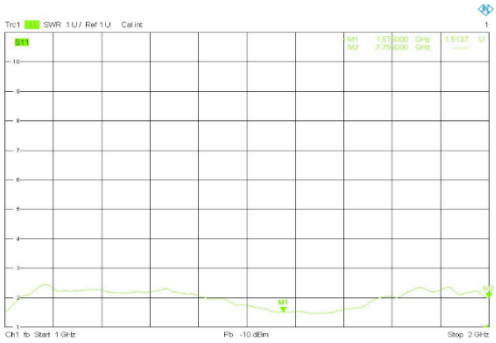

Fig 5. The SWR result 1575.42 MHZ Antenna

2-The Results of the 1195.192MHZ Helix

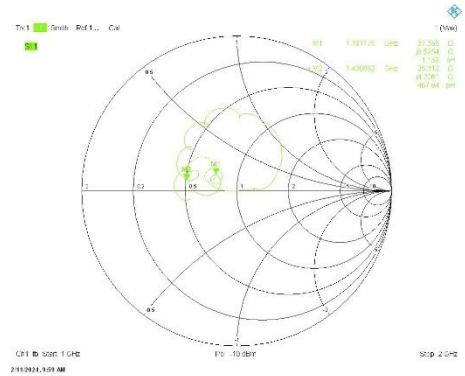

Fig 6. The Smith chart of 1195.192 MHZ Antenna

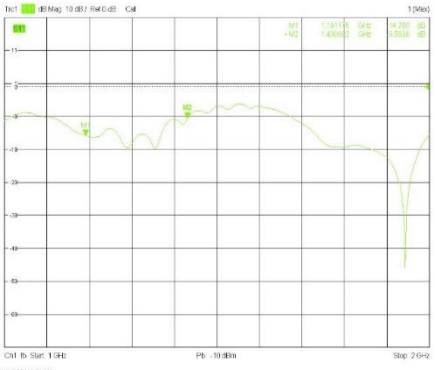

Fig 7. Return loss 1-2 GHZ

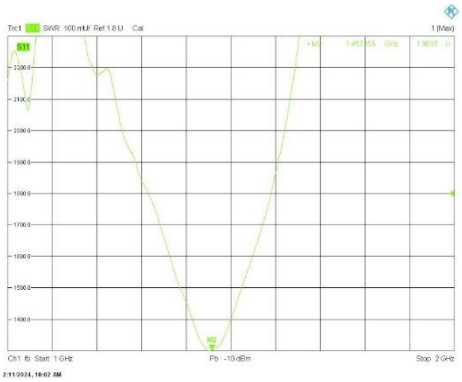

Fig 8. The SWR result 1195.192MHZ Antenna.

3. The Results of the 1455.1MHZ Helix

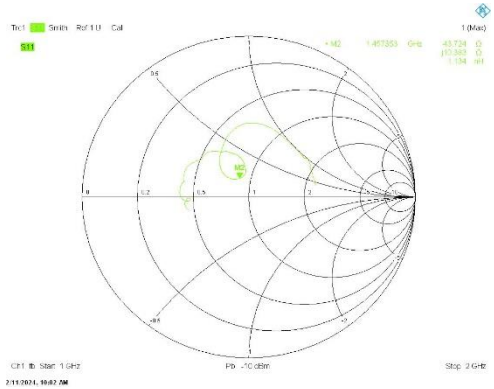

Fig 9. The Smith chart of 1455.1 MHZ Antenna

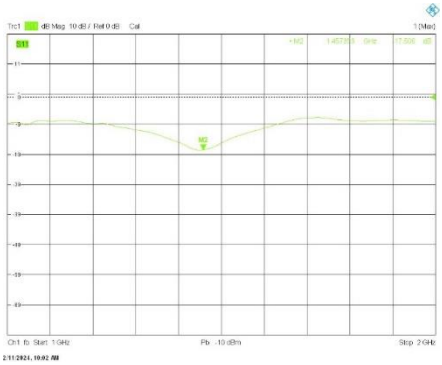

Fig 10. Return loss 1-2 GHZ

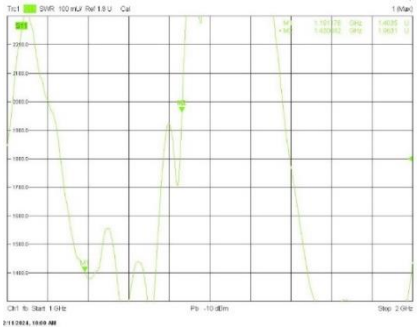

Fig 11. The SWR result 1455.1 MHZ Antenna.

4. The Results of the 1606 MHZ Helix

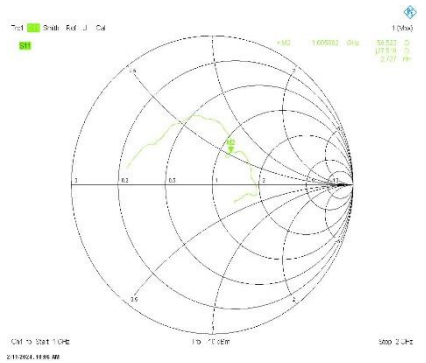

Fig12. The Smith chart of 1606 MHZ Antenna

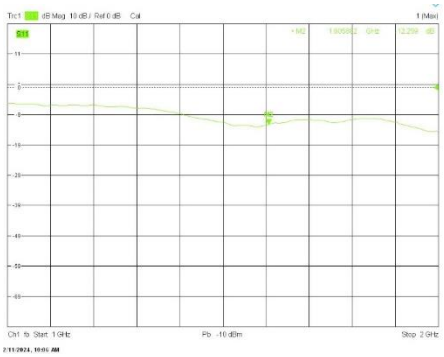

Fig 13. Return loss 1-2 GHZ.

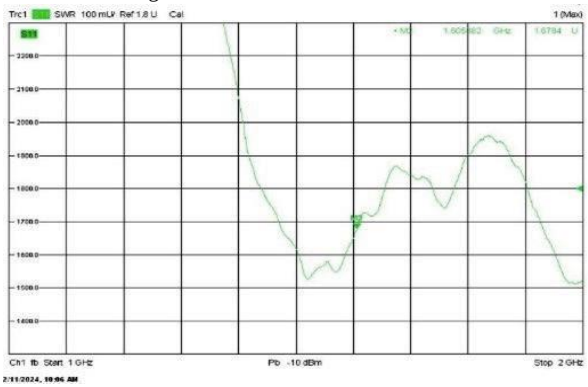

Fig 14. The SWR result 1606 MHZ Antenna

Method Of Connection:

We expressed the method of connection as show in fig.15.

1. Raspberry Pi 4B is Connected to Arduino uno and Camera via USB.
2. Arduino Uno is Connected to Motor Driver (DM556) Which is responsible of controlling stepper motor.
3. Motor Driver is Connected to Power Supply of 24V and 10A. Stepper Motor (Nema 34), Which has a holding torque of 40 kg.cm, is Also Connected to the Driver To ensure the accuracy and functionality of the motor.

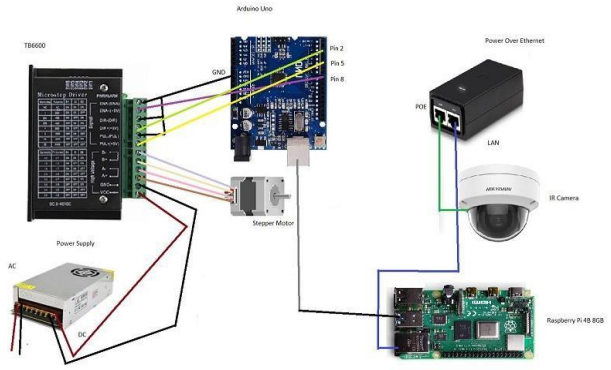

Fig 15. the connection of tracker syst

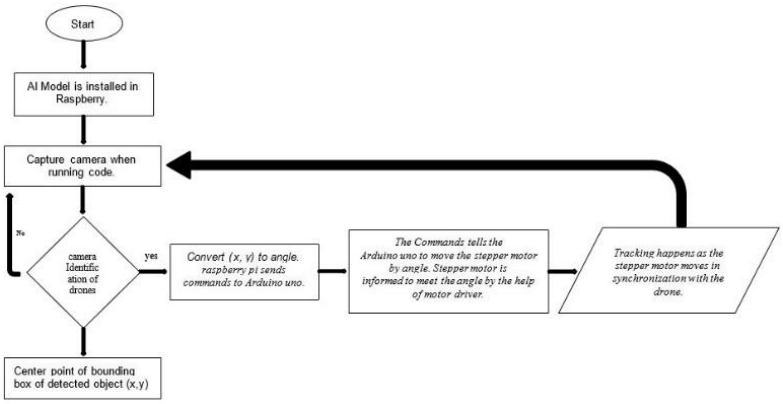

Fig 16. system flowchart

C. YOLO MODEL

One of the most important tasks in computer vision is object detection, which is locating and identifying items in an image or video. It serves as a foundation for various applications, ranging from autonomous vehicles and robotics to security systems and augmented reality. In recent years, the demand for real-time and accurate object detection has grown exponentially, necessitating the development of novel algorithms capable of meeting these requirements.

The You Only Look Once (YOLO) algorithm has emerged as a groundbreaking solution to real-time object detection. Unlike traditional multi- step approaches that rely on region proposal networks (RPNs) and subsequent refinement, YOLO follows a unified pipeline, processing the entire image at once to predict bounding boxes and class probabilities [10]. This unique design philosophy offers remarkable speed advantages, making it highly suitable for real-time applications

Detection model:

The YOLOv8 model is a state-of- the-art object detection algorithm that detects drones of different shapes and sizes. It outperforms previous YOLO versions in terms of accuracy and speed. The model is built using PyTorch and integrated with OpenCV for image processing and used to send control signals to these devices, allowing for seamless integration between the detection algorithm and the physical jamming mechanism [11].

Dataset preparation and training:

We collected a dataset of 4030 images of different drones' shapes and then split up into 70% training set and 30% validation set.

Then the model is trained through 100 epochs. During training, the model learns to identify and localize drones in images accurately. The loss function is minimized through backpropagation, resulting in improved detection performance over time.

Various evaluation metrics such as precision, recall, and mean Average Precision (mAP) are calculated to quantify the model's performance.

Results:

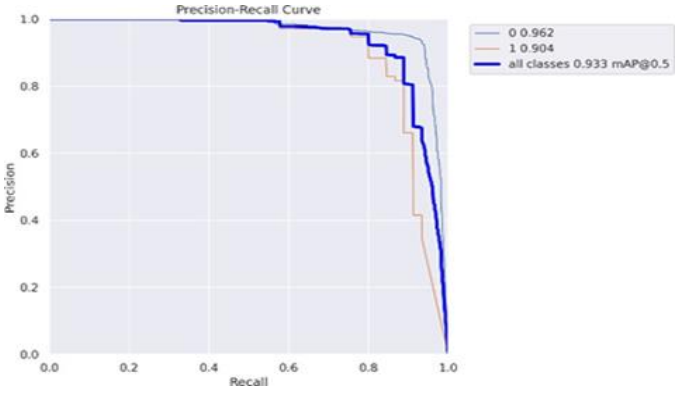

Fig.17. precision-recall curve

The curve is a precision-recall curve for the model. It shows the trade-off between the model's precision (the ability to correctly identify a drone) and its recall (the ability to find all the drones in an image).

The model has a high precision of 0.962 when the recall is 0.904. This means that for 90.4% of the drones in the image that the model detects, it is correct 96.2% of the time.

The mAP@0.5 value is 0.933. This stands for "mean Average Precision at an Intersection over Union (IoU) threshold of 0.5". IoU is a metric that measures how well a predicted bounding box overlaps with the actual drone in the image. An IoU of 0.5 means that the bounding box must overlap with the drone by at least 50% for it to be counted as a correct detection. The mAP@0.5 value of 0.933 means that the model has an average precision of

0.933 when the IoU threshold is set to 0.5.

Fig.18. recall-confidence curve

The curve is a recall-confidence curve for the model. It shows the trade- off between the model's recall (the ability to find all the drones in an image) and its confidence (how certain the model is that a detection is actually a drone). The model has high recall (0.904) at a reasonable confidence level (0.962).

This means that the model can find a large proportion of the drones in an image (90.4%) while still being fairly certain (96.2%) that they are actually drones.

The mAP@0.5 value is 0.933. This stands for "mean Average Precision at an Intersection over Union (IoU) threshold of 0.5". IoU is a metric that measures how well a predicted bounding box overlaps with the actual drone in the image. An IoU of 0.5 means that the bounding box must overlap with the drone by at least 50% for it to be counted as a correct detection. The mAP@0.5 value of 0.933 means that the model has an average precision of 0.933 when the IoU threshold is set to 0.5.

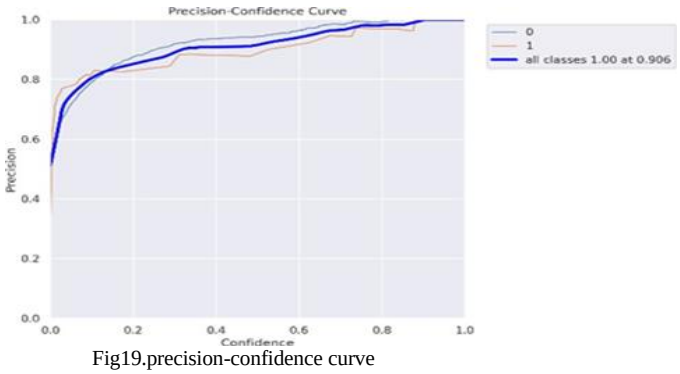

Fig19.precision-confidence curve

The curve is a precision-confidence curve. It shows the trade-off between the model's precision (the fraction of correct detections among all detections) and its confidence (how certain the model is that a detection is actually a drone).

The model has high precision (1.00) at a confidence level of 0.906. This means that when the model is very confident (confidence ≥ 0.906) in a detection, it is almost always correct (precision = 1.00).

The mAP@0.5 value is not provided in the image. However, we can see that the average precision across all confidence levels is close to 1.0, which suggests that the model is very good at making accurate detections.

the image shows a confusion matrix for the model

Confusion Matrix

Fig.20. confusion matrix

0.97: This value represents the True Positive Rate (TPR), also known as recall, which means 97% of the actual drones in the images were correctly identified by the model.

0.03: This value represents the False Positive Rate (FPR), which means 3% of the time, the model identified something as a drone when it wasn't actually a drone.

0.95: This value represents the True Negative Rate (TNR), which means 95% of the time, the model correctly identified non-drones as non-drones.

0.05: This value represents the False Negative Rate (FNR), which means 5% of the time, the model missed a drone and didn't identify it.

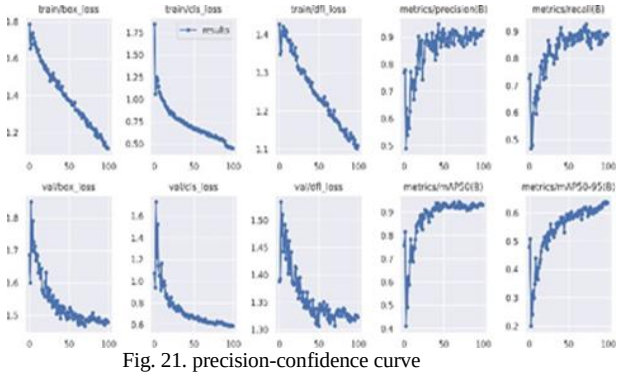

Fig. 21. precision-confidence curve

mAP@0.5: 0.933. This means the model has an average precision of 0.933 when the IoU threshold is set to 0.5.

Precision at recall of 0.904: 0.962.

This means that when the model recalls 90.4% of the drones (i.e., finds 90.4% of all actual drones), it has a precision of 96.2% (meaning 96.2% of its detections are correct).

mAP@0.95: 0.600. This means the model has an average precision of 0.600 when the stricter IoU threshold of 95% is applied.

Precision at recall of 0.5: 0.745. This means that when the model recalls 50% of the drones with the stricter IoU threshold, it has a precision of 74.5%.

The model seems to be performing well at detecting drones in images, with a high recall (97%) and a reasonable precision (around 0.933 at an IoU of 0.5). However, there is always room for improvement, and future work could focus on reducing the false positive rate (3%) and the false negative rate (5%).

SOLAR PANEL

In our setup, solar panels served as an emergency power source rather than the main source. These panels are made up of solar cells, which are essentially electronic devices that directly convert sunlight into electricity. When light hits a solar cell, it creates an electric current and voltage, which in turn generates electricity. There are two key things needed for this process: first, a material that can absorb light and boost the energy of electrons, and second, a way for these energized electrons to move from the solar cell to a usable circuit. The electron then loses its extra energy in the circuit before returning to the solar cell. While various materials and methods could potentially achieve this photovoltaic (PV) power conversion, almost all practical applications rely on semiconducting materials with a p-n junction. As we explore sustainable energy options like solar power, this article will delve into the different types of solar cells and their uses.

STUDY

The main components of solar panels are silicon solar panel consisting of union silicon cells that produce electrical energy.

SOLAR PANEL CONSISTS OF:

1. Solar cell

Solar cell in our project are silicon solar panel with 20-watt maximum power and 18-volt operating voltage and 30-volt max voltage and 1.11 max current.

2. Solar Charge Controller

A charge controller, also known as a charge regulator, is a crucial component in regulating the voltage and current from solar panels to batteries, preventing overcharging and damaging them. However, for small panels under 5 watts, a charge controller may not be necessary. In our project, we use a 12-to-24-volt, 5-amp charge controller.

3. Solar Battery

Solar panels generate excess electricity that can be stored in batteries as a backup power source. Lead-acid batteries are cost-effective and come in 12 or 24 volts. Proper battery system size considers voltage, current, and power. Our project uses a 12-volt, 7-amp-hour battery. [14]

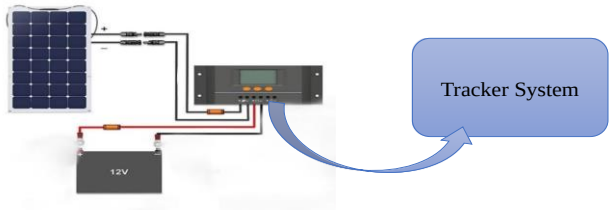

Fig. 22. Solar system with tracking system

IV. CONCLUSION

In conclusion, this research successfully developed and implemented a standalone high-gain jammer system for disrupting unmanned aerial vehicles (UAVs) operating on GNSS frequencies. The system achieved its objectives by utilizing strategically placed helix antennas, a YOLO-based tracking system for improved accuracy, and a reliable solar-powered standby system. Experimental evaluations demonstrated the effectiveness of the system in disrupting UAVs, highlighting its potential to enhance security in sensitive areas and protect critical infrastructure. This research contributes to the field of UAV countermeasures by offering a practical, efficient, and reliable solution for mitigating the growing threat posed by unauthorized drone activity. As shown in fig 23 Our project consists of two systems first one is a tracker system with camera look in random direction once it’s see UAV

it's give the information to raspberry pi and it's give command to Arduino to start motor motion in the same direction of camera because we have jammer system consist of directive antennas so when motor moves the jammer system in the direction of drone jamming Fig 24 The system is ready for jamming. accuracy will be higher than without tracking system In this picture we have mobile phone, and we open an drone figure on it and we move it right and left when the camera see this figure it's sending information to raspberry pi to send a command to Arduino to move the motor then jammer system will move in the direction of drone fig.24

Fig.23.the integraded system

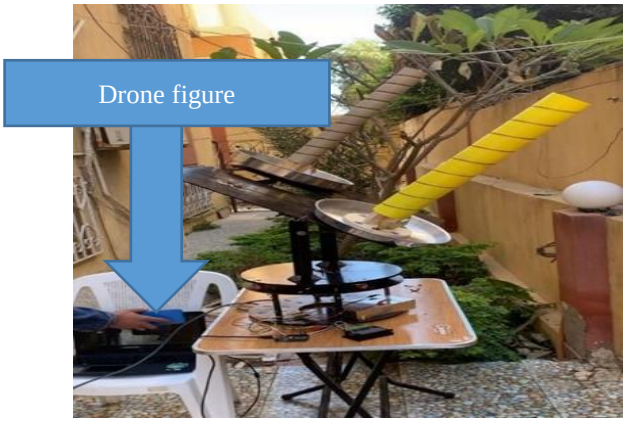

Fig.24. The antenna system moved in the drone direction.

V. ACKNOWLEDGEMENT

We would like to express our sincere gratitude and appreciation to Professor Dr. Mamdouh Gouda & Dr. Ashraf Samy and eng. Mohamed Abd Al Aleem for their invaluable guidance and support throughout the graduation project.

VI. REFERENCES

[1] Tomislav Milošević (2022), Jamming a Drone - EM Simulation of Simple EW and EW Countermeasures Scenarios, PROCEEDINGS, IX INTERNATIONAL CONFERENCE IcETRAN, Novi Pazar, Serbia

[2] J. Farlik, M. Kratky, and J. Casar, "Detectability and jamming of small UAVs by commercially available low-cost means," in Communications (COMM), 2016 International Conference on. IEEE, 2016, pp. 327–330.

[3] Kentsch, S., Caceres, M. L. L., Serrano, D., Roure, F., & Díez, Y. (2020). Computer vision and deep learning techniques for the analysis of Drone-Acquired Forest Images, a transfer learning study. Remote Sensing, 12(8), 1287. https://doi.org/10.3390/rs12081287

[4] Lee, M. R., & Chen, Y. (2023). Artificial intelligence-based object detection and tracking for a small underwater robot. Processes, 11(2), 312. https://doi.org/10.3390/pr11020312

[5] Ahmad, T., Ma, Y., Yahya, M., Ahmad, B., Nazir, S., & Haq, A. U. (2020). Object Detection through Modified YOLO Neural Network. Scientific Programming, 2020, 1–10. https://doi.org/10.1155/2020/8403262

[6]Joseph Redmon, Santosh Divvala, Ross Girshick, Ali Farhadi; Proceedings of the IEEE Conference on Computer Vision and Pattern Recognition (CVPR), 2016, pp. 779-788

[7]Gupta, C., Gill, N.S., Gulia, P. et al. A novel finetuned YOLOv6 transfer learning model for real-time object detection. J Real-Time Image Proc 20, 42 (2023).

[8] Kang, C.H., Kim, S.Y. Real-time object detection and segmentation technology: an analysis of the YOLO algorithm. JMST Adv. 5, 69–76 (2023). https://doi.org/10.1007/s42791-023-00049-7

[9] European GNSS Agency, (2019). European Global Navigation Satellite Systems (EGNSS) for drones' operations: white paper, Publications Office. https://data.europa.eu/doi/10.2878/52219

[10] Terven, J. and Cordova-Esparza, D. (2023). A Comprehensive Review of YOLO: From YOLOv1 to YOLOv8 and Beyond, MACHINE LEARNING AND KNOWLEDGE EXTRACTION.

[11] Reis, D. J., Kupec, J., Hong, J., & Daoudi, A. (2023). Real-Time Flying Object Detection with YOLOv8. arXiv (Cornell University). https://doi.org/10.48550/arxiv.2305.09972

[12] Fahrenburch, A. and Bube, R. 1983, Fundamentals of solar cells, Academic Press, New York.

[13] Solar Power & Battery Systems for Beginners by Michael Holt covers the basics of solar power systems, including charge controllers.

[14] Off Grid Solar: A handbook for Photovoltaics with Lead-Acid or Lithium-Ion batteries by Dandelion.